Comparative and temporal transcriptome analysis of peste des petits ruminants virus infected goat peripheral blood mononuclear cells

Siddappa Manjunath[a, f]
smanju712@gmail.com

Bishnu Prasad Mishra[a]
bpmishra_1@hotmail.com

Bina Mishra[d]
binachauhanmishra@hotmail.com

Aditya Prasad Sahoo[a]
rush2aditya@gmail.com

Ashok K. Tiwari[b]
aktiwari63@yahoo.com

Kaushal Kishore Rajak[c]
kaushalvirol@gmail.com

D. Muthuchelvan[c]
drchelva@gmail.com

Shikha Saxena[a]
shikhasaxenaivri@gmail.com

Lakshman Santra[a]
lakshman.ivri@gmail.com

Amit Ranjan Sahu[a]
dramitr.sahu@gmail.com

Sajad Ahmad Wani[a]
wanisajad759@gmail.com

R.P. Singh[d]
rpsingh@dr.com

Y.P. Singh[e,]
ypivri@gmail.com

Aruna Pandey[a]
arunabioinfo@gmail.com

Sonam Kanchan[a]
kanchansonam@gmail.com

R.K. Singh[a]

This is the author's manuscript of the article published in final edited form as:
Manjunath, S., Mishra, B. P., Mishra, B., Sahoo, A. P., Tiwari, A. K., Rajak, K. K., … Janga, S. C. (2017). Comparative and temporal transcriptome analysis of peste des petits ruminants virus infected goat peripheral blood mononuclear cells. Virus Research, 229, 28–40. https://doi.org/10.1016/j.virusres.2016.12.014

rks_virology@gmail.com

Gandham Ravi Kumar[a, *]
gandham71@gmail.com

Sarath Chandra Janga[f, g, h, **]
scjanga@iupui.edu

[a]Division of Veterinary Biotechnology, ICAR-Indian Veterinary Research Institute, Izatnagar, Bareilly, Uttar Pradesh, 243122, India

[b]Division of Biological Standardization, ICAR-Indian Veterinary Research Institute, Izatnagar, 243122, India

[c]Division of Virology, ICAR-Indian Veterinary Research Institute (IVRI), Mukteswar Campus, Nainital, Uttaranchal, 263138, India

[d]Division of Biological Products, (ICAR-)Indian Veterinary Research Institute, Izatnagar, Bareilly, Uttar Pradesh, 243122, India

[e]ARIS Cell, (ICAR-)Indian Veterinary Research Institute (IVRI), Mukteswar Campus, Nainital, Uttaranchal, 263138, India

[f]School of Informatics and Computing, Indiana University Purdue University, 719 Indiana Ave Ste 319, Walker Plaza Building, Indianapolis, IN 46202, United States

[g]Center for Computational Biology and Bioinformatics, Indiana University School of Medicine, 5021 Health Information and Translational Sciences (HITS), 410 West 10th Street, Indianapolis, IN, 46202, United States

[h]Department of Medical and Molecular Genetics, Indiana University School of Medicine, Medical Research and Library Building, 975 West Walnut Street, Indianapolis, IN, 46202, United States

*Corresponding author.

**Corresponding author at: School of Informatics and Computing, Indiana University Purdue University, 719 Indiana Ave Ste 319, Walker Plaza Building, Indianapolis, IN 46202, United States.

(Delete the this line)[1]ARIS Cell, Indian Veterinary Research Institute, Izatnagar, Bareilly, Uttar Pradesh, 243122, India.

Abstract

Peste des petits ruminanats virus (PPRV), a morbillivirus causes an acute, highly contagious disease – peste des petits ruminants (PPR), affecting goats and sheep. Sungri/96 vaccine strain is widely used for mass vaccination programs in India against PPR and is considered the most potent vaccine providing long-term immunity. However, occurrence of outbreaks due to emerging PPR viruses may be a challenge. In this study, the temporal dynamics of immune response in goat peripheral blood mononuclear cells (PBMCs) infected with Sungri/96 vaccine virus was investigated by transcriptome analysis. Infected goat PBMCs at 48 h and 120 h post infection revealed 2540 and 2000 differentially expressed genes (DEGs), respectively, on comparison with respective controls. Comparison of the infected samples revealed 1416 DEGs to be altered across time points. Functional analysis of DEGs reflected enrichment of TLR signaling pathways, innate immune response, inflammatory response, positive regulation of signal transduction and cytokine production. The upregulation of innate immune genes during early phase (between 2-5 days) ~~viz~~vi2. interferon regulatory factors (IRFs), tripartite motifs (TRIM) and several interferon stimulated genes (ISGs) in infected PBMCs and interactome analysis indicated induction of broad-spectrum anti-viral state. Several Transcription factors – IRF3, FOXO3 and SP1 that govern immune regulatory pathways were identified to co-regulate the DEGs. The results from this study, highlighted the involvement of both innate and adaptive immune systems with the enrichment of complement cascade observed at 120 h p.i., suggestive of a link between innate and adaptive immune response. Based on the transcriptome analysis and qRT-PCR validation, an *in vitro* mechanism for the induction of ISGs by IRFs in an interferon independent manner to trigger a robust immune response was predicted in PPRV infection.

Keywords: PPRV; PBMCs; RNA-sequencing; Transcriptome; Protein-protein interaction networks; Transcription factors

1 Introduction

Peste Des Petits Ruminants (PPR) is a viral disease of economic importance, causing an acute, highly contagious disease in small ruminants – goats and sheep (Banyard et al., 2010). Peste Des Petits Ruminants Virus (PPRV), the causative agent of PPR belongs to the genus *Morbillivirus*, family *Paramyxoviridae*. The disease causes severe economic losses in terms of high mortality (upto 90%) and morbidity (100%) affecting the productivity of sheep and goats in endemic regions (Singh et al., 2009; Banyard et al., 2010). Given its economic relevance and severity, the disease is classified as a World Organization for Animal Health (OIE) listed disease (Kumar et al., 2014a~~; Kumar et al., 2014~~b). Till today, only one serotype of Peste Des Petits Ruminants Virus (PPRV) is known to exist, but different isolates of PPRV belonging to four different lineages (with fourth lineage present in Asia) based on phylogenetic studies of partial 'N' and 'F' gene sequences have been reported (Kumar et al., 2014a,b; Albina et al., 2013). Few recent reports indicate that the Asian lineage is now present in Africa as well (Kwiatek et al., 2011). Live attenuated vaccines are used for control of PPR, which have proved to be quite safe and provide protection in natural hosts during mass vaccination programs. Among these live attenuated vaccines, Nigeria 75/1 and Sungri/96 have been widely used for the control of PPRV in Africa (Diallo et al., 1989) and India (Saravanan et al., 2010) respectively.

Sungri/96 vaccine, produced by continuous passage of Sungri/96 strain (Goat origin) in Vero cells, is widely used for vaccination in sheep and goats throughout India (Singh et al., 2010). A single dose of a PPR vaccine contains ~10^3 $TCID_{50}$ of Vero cell-attenuated PPRV and is believed to provide protective immunity in sheep and goats for several years (Kumar et al., 2014a,b). This robust immune response that results in protection of hosts after vaccination is attributed to strong cell-mediated immunity followed by humoral immunity, which, however, needs to be investigated (Kumar et al., 2014a,b; Sinnathamby et al., 2001). Even though unlikely, recently field isolate of PPRV (PPRV/Nanakpur/2012) was shown not neutralizing against vaccine strain (Sungri/96), raising concerns of the cross-protection of Sungri/96 vaccine virus against an emerging field virus (Kumar et al., 2014a,b), and making it all the more important to understand the complete mechanisms of immune protection induced by Sungri/96 PPRV vaccine strain.

Host defense response against the invading virus, starts with the recognition of specific, conserved molecular patterns on the viruses called pathogen associated molecular patterns (PAMPs). These viral PAMPs are detected by host pattern recognition receptors (PRRs) located extra-cytoplasmic (toll-like receptors – TLR3/7) or cytoplasmic (RIG-I like receptors (RLRs) – RIG-I, MDA-5) in the host cells (Jensen and Thomsen, 2012). The viral sensing by the TLRs or RLRs initiates signaling cascades that induce the expression of virus-responsive genes and pro-inflammatory cytokines, which in turn orchestrate innate immunity, chemokines, and co-stimulatory molecules that promote T-cell activation and specific immunity, restricting viral replication (Akira et al., 2006; Lazear et al., 2013). Many virulent viruses have evolved different mechanisms to evade host defense systems. On the other hand, vaccine viruses (live attenuated), which are widely used for mass vaccination programs, effectively induce early innate immune response, which further shapes the adaptive immunity giving a robust immune response (Kumar et al., 2014a,b).

PPRV is both lymphotropic and epitheliotropic in nature (Pawar et al., 2008). Peripheral Blood Mononuclear Cells (PBMCs) are widely used as standard *in vitro* model to study host-PPRV interactions as in other morbillivirus infections (Bolt et al., 2002; Iwasa et al., 2010; Manjunath et al., 2015). PPRV enters lymphoid cells through signaling lymphocyte activation molecule (SLAM), which is widely expressed on all immune cells (Pawar et al., 2008). PBMCs consisting of lymphocytes (T cells, B cells and NK cells), monocytes and dendritic cells play an important role in pathogen recognition and induce early innate immune response for host defense. PBMCs were used as an *in vitro* model to investigate the role of TLRs ~~–~~ 3 and 7, and cytokines in differential susceptibility of goat breeds and water buffalo to PPRV infection (Dhanasekaran et al., 2014). The PBMC transcriptome represents not only the primary immune function of leukocytes, but also displays transcriptomic shifts of other tissues and organs due to physiological and environmental alterations (Liew et al., 2006; Kohane and Valtchinov, 2012). Recently, transcriptome analysis of PBMCs infected with PPRV uncovered transcription factors modulating immune response (Manjunath et al., 2015). However, dynamics of immune response with time would help in an improved understanding of the anti-viral state established after PPRV vaccination. Hence in the present study, modulation of the immune response with time at the transcriptome level in goat PBMCs infected with Sungri/96 vaccine strain using RNA-Sequencing was determined. The results from this study indicate activation of TLR7/10, which stimulates effector molecules ~~–~~ interferon stimulated genes ~~*via*~~*via* interferon regulatory factors in interferon independent manner to provide an effective anti-viral response against PPRV infection.

2 Material and methods

2.1 Ethics statement and animals

The experimental procedures in the present study were approved by Institute Animal Ethics Committee (I.A.E.C No. F.1.53/2012-13-J.D.). Goat kids (5 months old) used for blood collection were housed in appropriate containment facilities with feed and water *ad libitum*.

2.2 Virus propagation and purification

The virus strain used in this study Sungri/96 (a vaccine strain) is widely used for vaccination throughout India. Vero cells available in the laboratory were propagated in Eagle's Minimum Essential Medium (EMEM) containing 10% fetal calf serum (FCS) at 37 °C under 5% CO_2. The Vero cells were seeded into 850 cm^2 roller culture bottles and then infected with Vero cell adapted Sungri/96 vaccine virus, at 0.1 multiplicity of infection (MOI). Infected roller cultures were incubated at 37~~°~~ °C under 5% CO_2 and monitored for cytopathic effect (CPE). The medium was changed with EMEM containing 2% fetal calf serum (FCS) once every two days. When the cells showed 70–80% CPE, the

virus was harvested by two cycles of freezing and thawing and stored at −80 °C and purified by banding on sucrose gradient (ultracentrifuged). The purified virus was titrated by estimating 50% tissue culture infective dose ($TCID_{50}$) using Vero cells in 96 well microtitre plate. The purified virus was tested for its infectivity in Vero cells and was used further for infection in goat PBMCs.

2.3 Screening of animals for PPRV antibodies

Goats were screened for PPRV antibodies using competitive ELISA (c-ELISA) serum neutralization test (SNT). Competitive ELISA for the detection of PPR antibodies was carried out as per the method of (Singh et al., 2004) using c-ELISA Kit (IVRI, Mukteshwar). PBMCs were isolated from blood collected from animals that showed SNT titre >1:8 and Percentage Inhibition (PI) value less than 40%.

2.4 Virus infection in PBMCs with PPRV and confirmation

Goat PBMCs were isolated using Histopaque-1077 (Sigma, USA) by density gradient centrifugation and seeded into four six well plates. Two plates served as control for 48 h and 120 h and two plates were used for infection with PPRV. PBMCs c.a 1 × 10^6 cells in RPMI-1640 were added to each well with 100 IU/ml penicillin, 100 µg/ml streptomycin and 10% foetal calf serum (FCS), infected with PPRV (Sungri/96) at 1.0 MOI and incubated at 37 °C in 5% CO_2 incubator for 1 h of adsorption. After 1 h of adsorption, the virus inoculum was removed, centrifuged to collect the lymphocytes that were washed with fresh RPMI medium and added back to the wells. Fresh RPMI medium was then added to wells and incubated. The control sample (mock-infected) on the other hand received just the RPMI medium. The infected cells were collected at 24 h p.i, 48 h p.i, 72 h p.i. and 120 h p.i., and viral load was quantified through N gene expression. Time interval 48 h p.i. was chosen as an early time point in the study to allow increased number of cells to be infected with PPR virus, as evident from the N gene expression by qRT-PCR in comparison to 24 h p.i. Though the N gene expression increased at 72 h p.i, we selected 120 h p.i., as its expression was found to be highest at this time point (data not shown). PPRV infection was further confirmed by morphological changes, reverse transcription polymerase chain reaction (RT-PCR) (Manjunath et al., 2015) and FACS at both 48 and 120 h p.i.

2.5 Flow cytometry analysis of PPRV infected PBMCs

Quantitative measurement of PPRV infected PBMCs at 48 h and 120 h p.i was measured using flow cytometry. For flow cytometry analysis, the cells were fixed in 4% paraformaldehyde (PFA), permeabilized with 0.2% Triton X and incubated for 1 h at room temperature with primary antibody (1:100) raised against the whole PPR virus (Sungri/96) in goats. The cells were then washed with PBS and incubated with anti-goat FITC conjugated secondary antibody (1:2000) for 1 h at room temperature. After incubation, cells were washed thrice with PBS and resuspended in 500 µl, 1X PBS. A total of 10,000 cells were examined using the FL1 channel of a flow cytometer. Number of infected cells (PPRV positive PBMCs) at 48 h and 120 h p.i. were analyzed using CellQuest software (BD Biosciences).

2.6 RNA extraction, library preparation and Illumina sequencing

An RNeasy® Mini Kit (Qiagen®, USA) was used to extract and purify RNA from control and infected samples at 48 h and 120 h p.i., as per the method recommended by the manufacturer. RNA concentration of the samples was determined by Nanodrop spectrophotometer (Thermo Fisher Scientific Inc., USA) and the quality was checked on Agilent Bioanalyzer 2100 (Agilent Technologies, Germany). RNA samples with RNA Integrity Number (RIN) ≥ 8 were processed for library preparation. The library was prepared using Illumina kit following the manufacturer's protocol. Approximately, 10 µg of total RNA from infected and control PBMCs was used to isolate mRNA using magnetic Oligo dT beads (Illumina) and the mRNA was purified using mRNA purification kit (Invitrogen). The purified mRNA from both the samples was then fragmented (100–400 bp) using divalent cations for 5 min at 94 °C. The double stranded cDNA was synthesized using Superscript Double-stranded cDNA Synthesis Kit (Invitrogen, Camarillo, CA) using random hexamers (N6) primer (Illumina). The cDNA synthesized was then subjected to end repair and phosphorylation using T4 DNA polymerase, Klenow DNA polymerase and T4 polynucleotide kinase (PNK). The end repaired cDNA fragments were then polyadenylated at the 3'end using Klenow Exo (3′ to 5′ exo minus, Illumina). Illumina paired end adapters were then ligated to the ends of the 3′ adenylated cDNA fragments. The adapters ligated cDNA was then enriched with PCR amplification using primer pairs (PE 1.0 and PE 2.0) (Illumina) catalyzed by Phusion DNA polymerase. The cDNA libraries prepared from both the control and the infected samples were sequenced on Illumina HiSeq 2000 platform according to the manufacturer's instructions. Illumina Sequencing was performed at Sandor LifeSciences, Pvt. Ltd. (Hyderabad, India).

2.7 Raw data preprocessing

Quality control and filtering of the high quality (HQ) sequencing data was done using NGS QC toolkit, a standalone program and an open source application (Patel and Jain, 2012) Further, subsequent processing of the data was performed using prinseq-lite software (Schmieder and Edwards, 2011) to remove reads of low quality (mean phred score <25) and short length (<50) for downstream analysis. The average total number of reads were c.a 40 million per sample. The average percentage of HQ bases was 92.68%. Further to find out whether the sequencing reads actually fall on specific targets (genes) and have sufficient coverage, TEQC package (Hummel et al., 2011) in R was used. The coverage and normalized coverage of five genes at both the time points is given in Fig. 1.

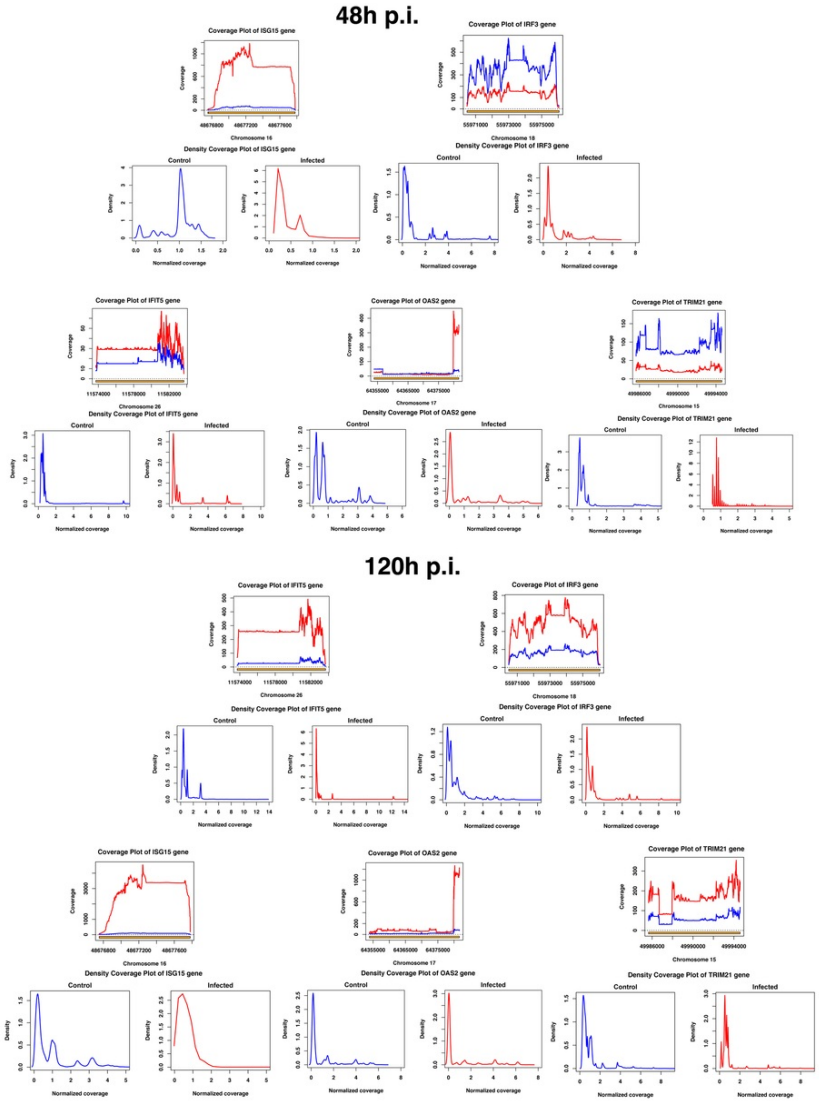

Fig. 1 Coverage and normalized coverage plots of five gene: Coverage and normalized coverage plots of IRF3, IFIT5, TRIM21, ISG15 and OAS2. The blue colour indicates the control and the red colour indicates the infected sample. (For interpretation of the references to colour in this figure legend, the reader is referred to the web version of this article.)

alt-text: Fig. 1

2.8 Viral transcript quantification

Reads from infected samples at both 48 h and 120 h p.i were mapped to the PPRV reference genome (GenBank: AJ849636.2) using bowtie 2.0 software (Langmead and Salzberg, 2012). The mapped reads for each viral transcript were then quantified by using Cufflinks in terms of fragment per kilobase of exon per million mapped reads (FPKM) using the PPRV gene transfer format (GTF) file downloaded from NCBI. The six viral transcripts (N-P-M-F-

H-L) were quantified and the differential expression of viral gene was represented as fold change between samples at 48 h and 120 h p.i respectively.

2.9 Identification of differentially expressed genes (DEGs) on comparative and temporal analysis and functional annotation

Fig. 2 summarizes the steps used in the analysis. Quality filtered reads from control and infected samples (48 h and 120 h) were mapped to the *Bos taurus* reference genome. *Capra hircus* genome is not well annotated therefore the well-defined *B. taurus* reference genome was used for mapping reads using TopHat version 2.0.7 (Kim et al., 2013). *Bos taurus* reference genome has been previously used by many groups for analyzing the goat transcriptome (Liu et al., 2013; Fontanesi et al., 2010). The mapped reads were then assembled using cufflinks, which quantifies the gene expression in terms of FPKM. DEGs at both the time points (48 h and 120 h p.i.) vis–a–vis their respective controls were identified by differential expression analysis – referred as comparative analysis in this study and the DEGs between the infected samples at 48 h and 120 h p.i., were identified by differential expression analysis – referred as temporal analysis in this study, using cuffdiff2 in cufflinks package (Trapnell et al., 2012). The significantly ($p \leq 0.05$) DEGs with ≥-±2 fold change were used for functional enrichment analysis using g:Profiler (Reimand et al., 2011) and Database for Annotation, Visualization and Integrated Discovery (DAVID) (Huang da et al., 2009). The common DEGs (243) among all the three conditions (I~~–48 h vs C–48 h; I–120 h vs C–120 h and I–48 h vs I–~~-48 h vs C-48 h; I-120 h vs C-120 h and I-48 h vs I-120 h ('I' stands for infected and 'C' stands for control)) were functionally profiled for biological processes and KEGG pathways using g:Profiler and DAVID. The DEGs functionally annotated to immune processes and common DEGs were further subjected to ClueGO analysis (Bindea et al., 2009) for functional enrichment in KEGG and REACTOME.

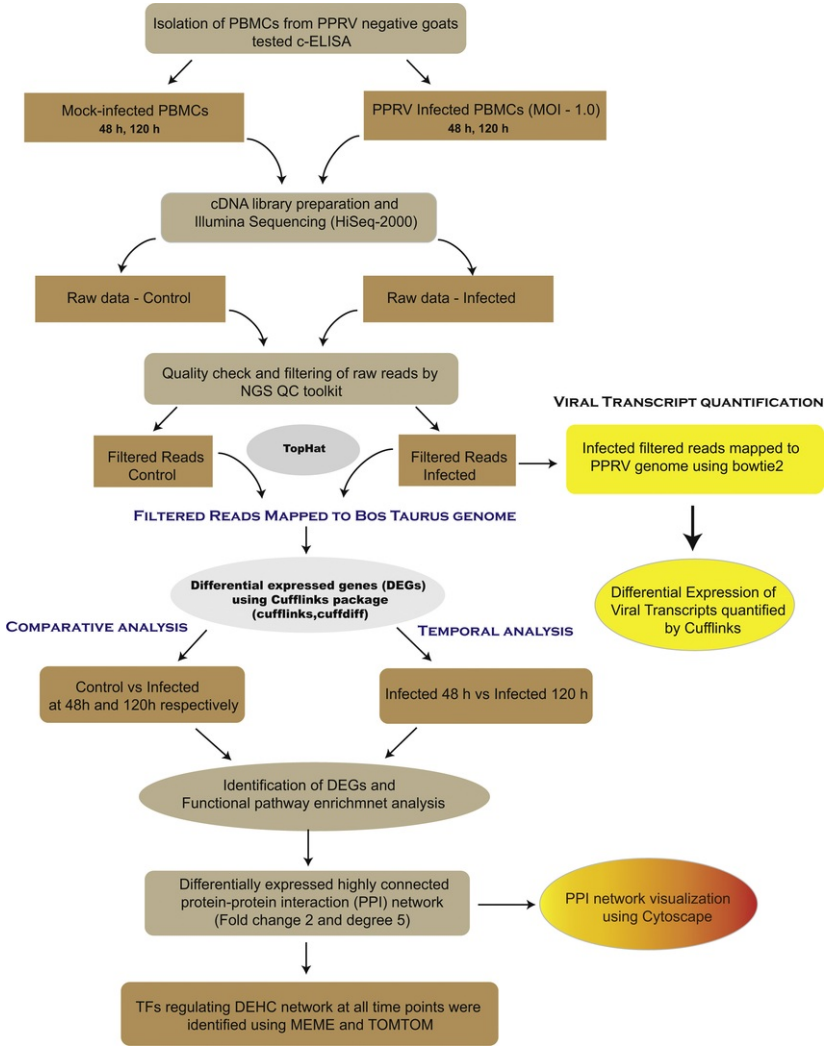

Fig. 2 Flow chart of steps depicting the analysis of transcriptome data starting from processing of raw reads, functional enrichment, protein-protein interactions networks (PPI) to identification of transcription factors (TFs) that bind to the upstream of the differentially expressed highly connected (DEHC) genes from comparative and temporal data analysis.

alt-text: Fig. 2

2.10 Protein–Protein interaction (PPI) networks of differentially expressed and highly connected genes (DEHC)

PPI network among all the DEGs from comparative and temporal analysis was retrieved using interactions available in the BioGRID database (Stark et al., 2006) and was found to be densely interconnected. The DEGs were then narrowed down based on fold change ≥±2 (Up- or down-regulated) and degree (calculated using igraph package (https://cran.r-project.org/web/packages/igraph/index.html)) ≥5 for both the conditions and were designated as differentially expressed highly connected (DEHC) genes. For comparative analysis at 120 h p.i., and 48 h p.i, 2000 and 2540 DEGs were narrowed down to 163 and 181 DEHC genes, respectively, and for temporal analysis 1416 DEGs were narrowed down to 126 DEHC genes. The PPI network for DEHC genes was visualized using Cytoscape software (Shannon et al., 2003).

2.11 Identification of transcription factors (TFs) regulating DEGs

TFs, binding to the upstream of DEHC genes from comparative and temporal analysis were identified by running MEME (Bailey et al., 2006). followed by TOMTOM (Gupta et al., 2007) tools from the MEME package. Initially, 5 kb upstream of DEHC genes for both the conditions were extracted from Ensemble BioMart and thirty overrepresented conserved motifs were identified using MEME (Multiple EM for Motif Elicitation) Suite. TFs binding to these motifs of DEHC genes for both the conditions (Comparative and Temporal analysis) were identified using TOMTOM. Orthologs of the TFs in *Bos taurus* were identified using g:orth in g:Profiler. The presence of these TF binding sites across the DEHC genes ~~are~~is shown as a heatmap using geneE software (Broad Institute).

2.12 Validation of RNA sequencing data using Quantitative Real time PCR (qRT-PCR)

A total of six genes of interest from both the analyses resulting from RNA sequencing data were selected for further validation. These genes were selected keeping in view the pathway that was predicted in the study. qRT-PCR was carried out on the same biological material that was used in RNA-Seq experiment on Applied Biosystems 7500 Fast system using 2X SYBR Green Master mix (USB, Sigma). GAPDH was identified as the stable reference gene from panel of housekeeping genes for normalization of target gene(s) of interest (Siddappa Manjunath et al., 2015). The primer sequences for the genes used for validation are given in Table 1. For all genes tenfold serial dilution were run in the study to estimate the efficiency of PCR, and the percentage efficiency ranged between 95 and 100%. Also, the expression of IFNs ~~-~~ α and β was also validated using custom TaqMan gene expression assays from Life Technologies. All the samples were run in triplicates. The relative expression of each sample was calculated using the $2^{-D\Delta CT}$ method with control group as calibrator (Schmittgen and Livak, 2008). Student's ~~t~~-test was done in JMP9 (SAS Institute Inc, Cary, USA) and differences between groups were considered significant at $p \leq 0.05$.

Table 1 Genes and their primer sequences used for validation of the RNA-sequencing data and prediction of immune signaling pathway.

alt-text: Table 1

Genes	Primer sequence	Accession Numbers
IRF3	Forward: AGCGTCCCTAGCAGACAAGA Reverse: CCAGGTTGAACACACCTCCT	JQ308793.1
ISG15	Forward: CAGTTCATCGCCCAGAAGAT Reverse: GTCGTTCCTCACCAGGATGT	XM_005690795.1
HERC5	Forward: GTATGAGGTTGGCTGGCATT Reverse: CCCTGACTCCTCCAAAATCA	XM_005681669.1
IFIT3	Forward: AAGGGTGGACACTGGTCAAG Reverse: AGGGCCAGGAGAACTTTGAT	XM_005698196.1
IFIT5	Forward: CTTGGAGGTGACACCAACCT Reverse: CCACAGCTGCTTTGAAATGA	XM_005698239.1
IRF7	Forward: GACACGCCCATCTTTGACTT Reverse: ACTGTCCAGGGAGGACACAC	XM_004019737.2

3 Results

Goats (5~~-~~6 months old) screened −ve for PPRV antibodies by competitive ELISA (c-ELISA) were selected for collection of blood. The goat PBMCs were infected with purified PPR vaccine virus (Sungri/96) at 1.0 MOI and were observed for morphological changes from 24 h to 120 h p.i. The infected cells showed ballooning and clumping of cells from 48 h p.i with progressive increase in cytopathic effect (CPE) at 120 h p.i (Fig. 3A). No such changes were observed in uninfected cells. Amplification of 351 bp fragment of N gene of PPRV in infected goat PBMCs at 48 h and 120 h p.i., confirmed PPRV infection in PBMCs (Fig. 3B). The cells (PBMCs) infected with PPRV were quantified further by flow cytometry using polyclonal serum raised in goats against PPRV (Sungri/96) vaccine virus. The percent infected PBMCs were found to be 49.31% and 72.72% at 48 h p.i and 120 h p.i., respectively (Fig. 3C). The viral transcripts were quantified using PPRV reference genome at 48 h and 120 h p.i. The results showed increase in expression of Nucleoprotein (N) gene followed by fusion (F), Haemagglutinin (H), Large (L), Matrix (M), and Phosphoprotein (P) with time (Fig. 3D). These results ratified progression of PPRV infection from 48 h to 120 h p.i.

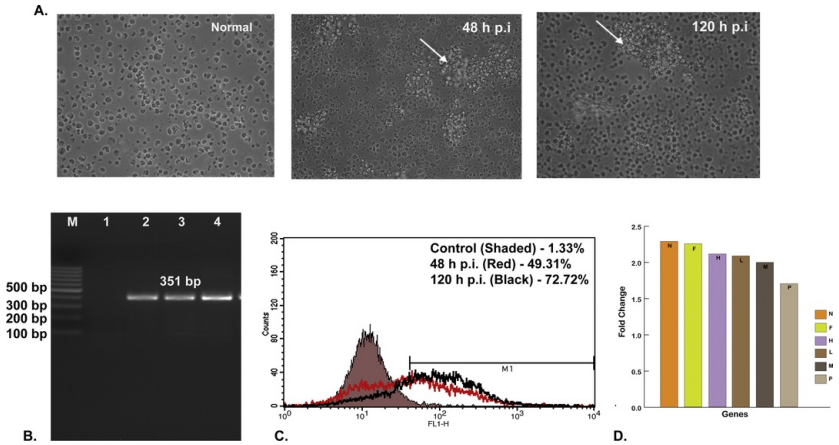

Fig. 3 Confirmation of viral infection and viral transcript quantification: (a). Morphological changes in infected PBMCs at 48 h and 120 h p.i., showing clumping of cells. The clumping of cells increased at 120 h p.i. (b). N gene amplification (amplicon size 351 bp) of PPR virus from infected PBMCs confirming infection at 48 h and 120 h p.i (Lane 2 & 3), Negative control (Lane 1), M- 100 bp Ladder; (c). Flow cytometry of infected cells at 48 h and 120 h p.i., using antibodies raised against the PPRV Sungri/96 whole virus. The number of cells infected increased with time from 48 h p.i to 120 h p.i (d). PPR viral gene transcript quantification at 48 h and 120 h p.i. N gene expression increased as the infection progressed followed by F, H, L, M, and P gene expression

alt-text: Fig. 3

3.1 Identification of DEGs on comparative and temporal analysis and functional annotation

Gene expression for comparative analysis was quantified at both the time points (48 h and 120 h p.i.) in terms of FPKM using cufflinks. A total of 2540 (48 h) and 2000 (120 h) genes were significantly ($p \leq 0.05$) differentially expressed at a fold change ≥~~±~~±2. A total of 797 DEGs were found commonly differentially expressed at both time points. At 48 h p.i, among the 2540 genes, 1130 were upregulated and 1410 genes were downregulated. At 120 h p.i., out of 2000 significant DE genes, 728 genes were upregulated and 1272 genes were downregulated. Temporal data analysis (I~~-120 h vs I-~~120 h vs I-48 h) of the infected samples revealed 1416 significantly ($p \leq 0.05$) DEGs out of which 821 genes were upregulated and 595 genes were downregulated with fold change ≥~~±~~±2.

Significant gene ontology terms of 2540 (48 h p.i.) and 2000 (120 h p.i.) DEGs from comparative analysis were retrieved using g:Profiler and DAVID databases. DEGs were annotated to several gene ontology (GO) categories belonging to the three branches of ontology ~~–~~- biological process, molecular function, and cellular component. Under biological processes, significant enrichment of DEGs at 48 h p.i.,was seen for immune system processes, cytokine production, TLR signaling pathway, IL-6 production, regulation of T-cells, etc. Whereas, at 120 h p.i., immune system process, regulation of cellular process, defense response etc., were found to be enriched. A total of 297 (p-value = 1.20E-20) and 238 genes (p-value = 3.19E-21) at 48 h and 120 h p.i., respectively, were involved in immune system processes with significant enrichment. Under the molecular function category, cytokine activity, kinase activity, cytokine receptor binding and chemokine receptor binding, were enriched at both time points. A number of DEGs at these time points were found to be localized on the cell surface, cell membrane, cytosol and vesicles under cellular component category. To further define DEGs function in goat PBMCs following PPRV infection the biological pathways enriched in the infected transcriptome at these time points were analyzed using KEGG pathways in DAVID database. A total of 597 genes with 15 significant ($p \leq 0.05$) categories at 48 h p.i., and 426 genes with 13 significant categories at 120 h p.i. were found to be mapped to the reference canonical pathways in KEGG. The most significant KEGG pathways represented by most of the DEGs were cytokine-cytokine receptor interaction, NOD like receptor signaling pathway, haematopoietic cell lineage and Toll-like receptor signaling pathway at both time points. In addition, enrichment of complement cascade was observed at 120 h p.i. suggesting it as a link between innate and adaptive response.

The DEGs functionally annotated to immune processes by g:Profiler at 48 h p.i and 120 h p.i. respectively, were further subjected to ClueGO analysis. At 48 h p.i, TLR3/7/8 signaling cascades, activation of interferon regulatory (IRF) pathways, cytokine signaling, RIG-I/MDA5 pathways, NF-kB activation, ISG15 antiviral signaling, etc., were significantly ($p \leq 0.05$) enriched (Fig. 4A). At 120 h p.i., all these pathways were found to be more enriched than 48 h p.i. as represented by the size of the node (*p* Value corrected with Bonferroni step down) in addition to B-cell receptor signaling and T-cell receptor signaling pathways (Fig. 4B). Similarly, the immune genes identified on temporal analysis showed significant ($p \leq 0.05$) enrichment of TLR signaling pathway, RIG signaling pathway, chemokine signaling pathway, Class-I MHC presentation and processing, and classical antibody mediated complement activation, etc., (Fig. 4C). The enrichment of these pathways in temporal analysis clearly indicated that the immune response was progressing from innate to adaptive with time.

Fig. 4 ClueGO analysis of the Immune genes identified from comparative analysis and temporal analysis. A. 48 h p.i. comparative analysis B. 120 h p.i. Comparative analysis C.Temporal analysis. The GO terms are represented as nodes. The gradient from red to green indicates the percent associated genes and the diameter of the node is the P Value corrected with Bonferroni step down. (For interpretation of the references to colour in this figure legend, the reader is referred to the web version of this article.)

alt-text: Fig. 4

Further, the functional profiling of 1416 DEGs from temporal analysis showed enrichment of immune system, defense response, innate immune response processes and cytokine interactions etc., indicating that the host defense was responding by activating its immune response genes and its signaling pathways as the infection progressed. In addition, some of the biological processes like cell adhesion, cell motility and pathways involved in cell adhesion, focal adhesions, adherens junctions, etc., were enriched indicating that the cytoskeleton and cell to cell communications were affected as PPRV infection progressed.

The common DEGs (243) among comparative and temporal analysis were also functionally enriched using g:Profiler and DAVID. The common DEGs also showed enrichment for biological processes like immune system process, inflammatory response, positive regulation of signal transduction, cytokine production, MAPK cascade, and innate immune response. The enriched pathways for KEGG showed cytokine-cytokine receptor interaction, phagocytosis and immunoglobulin production as important pathways suggesting the involvement of both innate and adaptive immune systems. Further, on ClueGO analysis of these DEGs, enrichment of TLR signaling pathway, RIG signaling pathway, Class-I MHC presentation and processing, chemokine signaling, B and T-cell receptor signaling pathways, also indicated the role of both innate and adaptive immune responses in PPRV infected PBMCs (Fig. S1 in Supplementary data).

3.2 DEGs and broad spectrum anti-viral response

Among the DEGs identified on comparative analysis, Toll like receptor 7(TLR7), which is activated by single stranded (ss) RNA virus, was upregulated at 120 h p.i., and TLRs – 2, 4, and 8 were downregulated at 48 h p.i. Among the IRFs – IRF7 at 48 h p.i, and IRF 3, 7 and 9 at 120 h p.i., which orchestrate and maintain the homeostatic mechanism of the host defense, were upregulated compared to the uninfected controls. IRF3 and IRF7 play an essential role in induction of Type I IFNs (IFN-α/β), but these IFNs were not expressed in PPRV infected PBMCs at both time points. Also, the broad-spectrum anti-viral IFN-induced proteins with tetratricopeptide repeats – IFIT3 and IFIT5 were upregulated at both time points and IFN-induced transmembrane proteins – IFITM1 and IFITM2 were upregulated at 120 h p.i. The tripartite motif family of proteins involved in regulation of innate immune system

processes through modulation of PRR signaling pathways and inhibition of virus entry, ~~vir~~vi2. TRIM21, TRIM34, TRIM25, TRIM5 and TRIM56 at 48 h p.i. and TRIM25, TRIM56, TRIM2 and TRIM36 at 120 h p.i., were all found to be upregulated. Oligoadenylate synthetases ~~–~~ OAS1Z, OAS1X and OAS1Y that respond to viral PAMPs by inducing degradation of viral and cellular RNAs to block viral infections were upregulated at both time points and OAS2 was upregulated at 120 h p.i. ISG15 (Interferon stimulated gene 15), which acts as critical anti-viral molecule in many RNA viral infections (Influenza, hepatitis C, HIV-1, etc.) was upregulated at both 48 h p.i (36.5 folds) and 120 h p.i. (36.75 folds). Mx1 and Mx2 – inhibitors of viral entry were upregulated at 48 h p.i., and Viperin (RSAD2), an antiviral effector and HERC5, a positive regulator of innate antiviral response were upregulated at both time points. Bcl-6 and Bcl-2, which are anti-apoptotic, were found to be upregulated at 48 h p.i and 120 h p.i., respectively. The other Bcl-2 family of proteins like BCL2L1 and BCL2L2~~-~~ – anti-apoptotic; and BCL2L14 and BCL2L15 – pro-apoptotic, were found to be downregulated. BAG3 and BIRC5 (anti-apoptotic factors) were found to be upregulated at 48 h p.i. and 120 h p.i. All the important innate immune proteins ~~vir~~vi2. interferon regulatory factors (IRFs), tripartite motifs (TRIMs) and interferon stimulated genes (ISGs), which act as first line of host defense against the invading viruses were all found to be significantly upregulated at both time points.

Among other significantly expressed DEGs, Vimentin (VIM), an intermediate filament responsible for maintaining cell shape and integrity and involved in immune response, and actin binding proteins, coronins ~~vir~~vi2. CORO1B, CORO1C and CORO2A, involved in cell cycle progression, and signal transduction and apoptosis, were downregulated at both time points. Beta-actin, the housekeeping gene that is constitutively expressed in all the cells and widely used as an endogenous control in a variety of experiments was found to be downregulated at 120 h p.i. This ratified our previous qRT-PCR results, which showed variable expression of beta-actin in PBMCs infected with PPRV (Manjunath et al., 2015). This suggested downregulation of cytoskeletal proteins due to PPRV infection in the infected PBMCs.

On temporal analysis, TLR10, an important innate immune sensor of viral infection; interferon response genes like IRF8, IFN-induced transmembrane proteins – IFITM2 and IFITM3, and OAS2, which restrict viral replication and confer basal resistance to viruses; and complement C2, C1QA, C1RL, etc., were all upregulated. The results of temporal analysis corroborated with the results of comparative analysis indicating that both innate and adaptive immune system were activated to establish an anti-viral state as PPRV infection progressed.

3.3 Protein-protein interaction network of DEHC genes

BioGRID database was used to predict the interactions for DEHC genes from comparative and temporal analysis. The protein-protein interaction network (PPI) of DEHC genes at 48 h p.i and 120 h p.i., showed 299 and 315 interactions, respectively. ISG15, an interferon stimulated gene, was found to be highly connected interacting with IFIT3, IFIT5, TRIM25, MX1, HERC5 and USP2 at 48 h.p.i, and IRF3, IFIT3, IFIT5, HSPA1A, EIF2AK2 and USP18 at 120 h p.i. (Fig. 5a and b). IRF3, a transcriptional regulator at 120 h p.i, was found to be connected to HERC5, IKBKE, ISG15 and TLR2 among the DEHC genes. Besides these genes, IRF3 was also connected to TRIM21 among the DEGs. IRF7, another key transcriptional regulator was connected to CREBBP, EAF1, IQSEC1, GCLM, UBC, TRAF6 and TLK2 at 48 h p.i, and SMAD3 and IRF3 at 120 h p.i., among the DEGs. The DEHC interaction network on temporal analysis resulted in 263 interactions, with C2 (complement) being the highly connected node with a degree of 49. C2 was well connected to CD4, HDAC10, HDAC11, CCL2, MAP3K5, etc. This suggested involvement of complement in linking adaptive and innate immunity as the PPRV infection progressed with time (Fig. 5c).

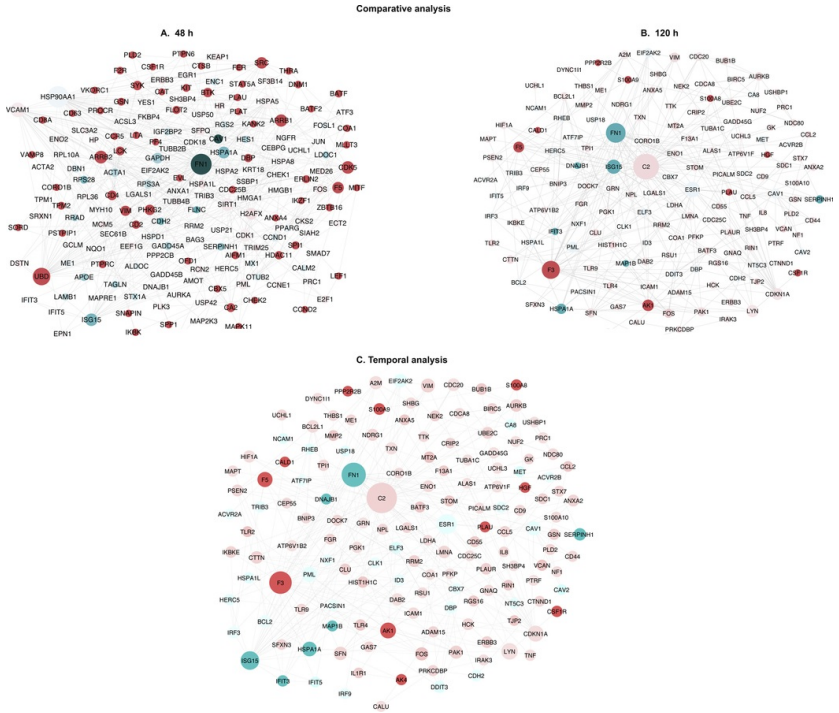

Fig. 5 Protein-Protein Interaction (PPI) networks for differentially expressed highly connected (DEHC) genes from comparative and temporal analysis: (a). Protein-protein interaction (PPI) network for DEHC genes at 48 h p.i on comparative analysis. (b). Protein-protein interaction network for DEHC genes at 120 h p.i on comparative analysis. (c). Protein-protein interaction (PPI) network for DEHC genes on temporal analysis.The upregulated genes are shown in green and downregulated genes are shown in red with the gradient showing the extent of expression. The size of the node indicates connectivity (~~*i.e. degree)*~~ *i.e.* degree). (For interpretation of the references to colour in this figure legend, the reader is referred to the web version of this article.)

alt-text: Fig. 5

3.4 Transcription factors co-regulating the DEHC genes

TFs modulating the expression of DEHC genes from comparative analysis at 48 h p.i and 120 h p.i were identified as described in materials and methods. Likewise, TFs for the DEHC genes from the temporal analysis were also identified. At 48 h p.i., 82 TFs were identified to control 126 DEHC genes. Among these predicted TFs, a total of 6 TFs (ETS1, FOXO3, GLIS2, MAFF, NKX3-1, NR2E1) at 48 h p.i were found to be dysregulated among the DEGs (Fig. S2 in Supplementary data). Among these, ETS1 (controls the differentiation of lymphoid cells and induction of cytokine and chemokine genes) and NR2E1 (involved in retinoic receptor regulation) were downregulated and FOXO3 (central regulator of innate immune function and regulate CD8 T-cell response in viral infection), GLIS2 (Role in kidney architecture and functions), MAFF (involved in cellular stress response) were upregulated. At 120 h p.i, 72 TFs were identified binding to the upstream of 117 DEHC genes (Fig. S2 in Supplementary data). Out of these, 5 TFs – CREB3L1, EBF1, IRF3, SP1 and VDR were dysregulated among the DEGs at 120 h p.i. CREB3L1 (which plays an important role to prevent viral spreading by inhibiting proliferation of virus-infected cells), EBF1 (involved in B-cell signaling), IRF3 (important anti-viral molecule) and SP1 (involved in immune response and apoptosis at later stage of infection) were all upregulated, whereas VDR (Vitamin D receptor) was found to be downregulated. In temporal analysis, a total of 70 TFs were identified binding to 77 DEHC genes. Among the predicted TFs for temporal analysis, 2 TFs were found to be dysregulated among the DEGs (EGR3 and NKX3-1). EGR3 regulating B and T-cell function in adaptive immune responses was upregulated, asserting the regulation of both humoral and cell mediated response genes as infection progressed (Fig. S3 in Supplementary data).

3.5 Validation of RNA sequencing data qRT-PCR

Six DEGs (IRF3, IRF7, IFIT3, ISG15, TRIM56 and HERC5) having an important role in immune regulation and anti-viral response were validated for their expression using real time qRT-PCR (Fig. 6). The expression of these DEGs was in concordance with RNA sequencing results. The expression of IFNs – α and β was found to be non – significant at both the time points (Fig. S4 in Supplementary data).

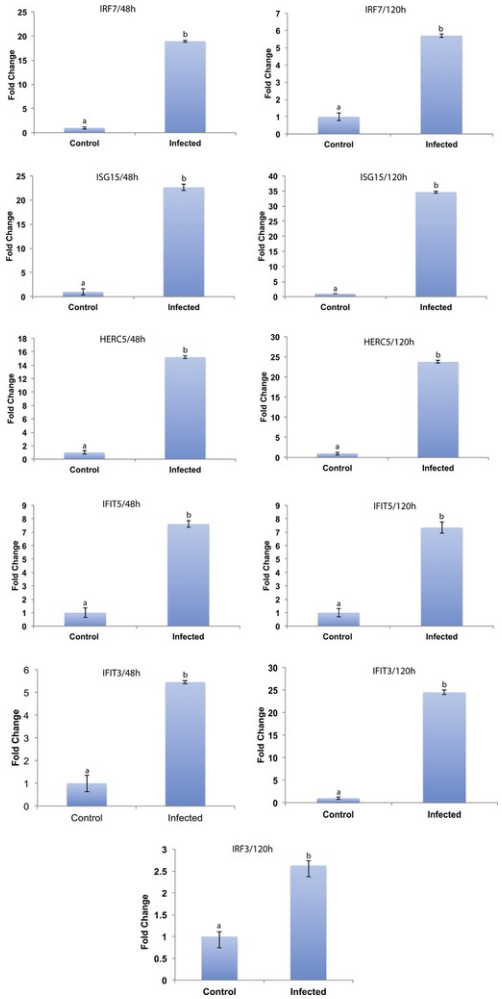

Fig. 6 Quantitative real-time PCR to validate the RNA-seq experiment. Fold change ($2^{-\Delta\Delta CT}$) with control as the calibrator is represented along with the standard error of difference. Levels not connected by same letter are significantly different.

alt-text: Fig. 6

4 Discussion

In the present study, goat PBMCs were infected with Sungri/96 vaccine virus and harvested at 48 h p.i and 120 h p.i. PBMCs transcriptome was evaluated to identify the global gene expression changes at 48 h p.i. and 120 h p.i, to understand and delineate the mechanism of early immune protection induced by the vaccine virus.

Functional annotation of the significant ($p \leq 0.05$) DEGs at 48 h and 120 h p.i (comparative analysis) showed enrichment of pathways, which were also observed to be enriched in other RNA virus infections reported earlier in several studies (Kuchipudi et al., 2014; Jin and Zou, 2013; Chakrabarti et al., 2010; Boon et al., 2011). Innate immune system is stimulated once the TLRs are engaged with PAMPs (Girardin et al., 2002). TLRs – 3, 7 and 8 are mainly involved in the recognition of the viral products (dsRNA and ssRNA viruses) and subsequently initiate cellular response to infection ~~via~~ *via* signaling pathways leading to early events in immune response (Alexopoulou et al., 2001; Diebold et al., 2004). In the present study, TLR7 was upregulated, and TLR- 3 & 8 were downregulated at 120 h p.i., and TLRs – 2, 4, 6 and 8 were downregulated at 48 h p.i. The downregulation of pattern-recognition receptors (TLRs), capable of sensing the presence of RNA virus, provides a mechanism by which the virus could evade host innate anti-viral responses (van Gent et al.,

2011). Also, on temporal analysis, TLR10 was found to be upregulated as the infection progressed. It was observed recently that activation of TLR10 by functional RNA-protein complex of influenza virus leads to robust induction of cytokine expression (Lee et al., 2014). Thus, in PPRV infection TLR7 and TLR10 may play an important role in triggering the downstream immune signaling networks.

ISGs are induced by viral infection to establish an antiviral state, both directly (by IRF3 after PAMP detection and PRR signaling) and indirectly (by IFN-β production and IFNAR signaling) with the later occurring in both infected and uninfected cells (Lazear et al., 2013). The absence of expression of type-I interferons in our study suggested that the stimulation of ISGs could be IFN independent and IRF dependent, which needs further investigation. These investigations may be possible with early and close sampling frames. This though reported in other paramyxovirus infections (Nanda and Baron, 2006), is an important observation not reported previously for PPRV infection. Previously, non-structural proteins (C, V and W proteins) of paramyxoviruses were shown to inhibit the induction of type I interferons in different cell lines (Boxer et al., 2009; Nanda and Baron, 2006). IRFs upregulated in the present study (IRFs – 3, 7, 8 and 9) were found to stimulate ISG15 by more than 30 folds at both time points. ISG15 is an early induced, important innate immune protein with broad anti-viral activity (Harty et al., 2009). This ISG15 can covalently be coupled to many host cellular proteins (a process known as ISGylation), often modulating their functions (Durfee et al., 2010). Antiviral activity associated with protein ISGylation *in vitro* and *in vivo* has been reported for both DNA and RNA viruses, including influenza A and B, Sindbis, vesicular stomatitis virus, respiratory syncytial virus and Ebola virus (Sadler and Williams, 2008; Sen and Sarkar, 2007; Osiak et al., 2005). ISG15 also conjugates with some viral proteins, such as NS1 protein of influenza, thereby inhibiting viral replication (Zhao et al., 2010). Other ISGs like IFITM2 and IFITM3 were also found to be upregulated in PPRV infected PBMCs. The protective roles of IFIT3 and IFIT5 were reported in avian influenza (Vanderven et al., 2012) dengue virus (Hsu et al., 2013) and other RNA virus infections thus, reasserting their possible role in PPRV infection.

TRIM family of proteins, positively modulate innate immune signaling pathways triggered by pattern recognition receptors (Akira et al., 2006; McNab et al., 2011; Gack et al., 2008; Tsuchida et al., 2010). In this study, TRIM21, TRIM25 and TRIM56 were upregulated at both the time points. TRIM21 is significantly induced and interacts with IRF3 upon RNA virus infection and the host antiviral responses are significantly boosted or crippled in the presence or absence of TRIM21 (Yang et al., 2009). TRIM14 and TRIM45 were found to be upregulated in temporal analysis as the PPRV infection progressed. Recently, it was observed that TRIM14, a component of mitochondrial anti-viral immunity recruits NF-kB essential modulator (NEMO) to MAVS complex inducing innate immune response mediated *via* RIG-I in influenza virus infection activating IRF3 and NF-kB (Zhou et al., 2014). TRIM14/21 may act as possible adaptors between PRRs (TLR/RIG-I) and activation of IRF3/IRF7 resulting in efficient cellular anti-viral response in PBMCs infected with Sungri/96 PPRV vaccine virus.

4.1 Predicted Immune signaling pathway triggered by Sungri/96 vaccine virus

Based on the RNA sequencing data analysis and qRT-PCR validation of important immune molecules, an immune signaling pathway that is triggered following inoculation of Sungri/96 PPR vaccine virus *in-vitro* was predicted (Fig. 7). PPR virus enters cells through specific receptor(s) on the surface of the host cell. SLAM an established receptor (Adombi et al., 2011) for PPRV (fold change >2 at 48 h p.i), expressed at 48 h p.i and not at 120 h p.i., may act as an entry receptor in initial stages of PPRV infection. CD46 that acts as a receptor for vaccine strain of measles virus is downregulated under infection from the cell surface (Tatsuo and Yanagi, 2002). This was found to be downregulated at 120 h p.i., in our study, suggesting CD46 as a possible alternate co-receptor for PPRV, apart from SLAM, which needs to be further investigated. Once the PPR virus enters the cells through its specific receptor(s) it is endocytosed and due to the acidic environment of the endosomes the viral nucleic acid is released. TLR7, found on endosomal surface recognizes negative (−) sense single stranded (ss) RNA and is activated as indicated by its upregulation. TLR7 once engaged with its ligand (ssRNA viral genome) activates first line of defense molecules called IRFs mainly IRF3 and IRF7 (Collins et al., 2004) which are upregulated in PPRV infected PBMCs. IRFs present in the cytoplasm translocates into the nucleus on phosphorylation, catalyzed by IKK family of kinases (Collins et al., 2004). The IKBKE expressed in the present study catalyzes phosphorylation of IRFs that translocate into the nucleus. Also, adapters play a role in linking TLR activation and IRFs (van Gent et al., 2011). TRIM14/21 that are significantly upregulated, act as possible adapter(s) in this study to activate IRFs. The phosphorylation of IRFs, prevents the interaction of IRFs with Pin1, which otherwise causes ubiquitination leading to complete degradation (Hiscott, 2007). IRFs translocated into the nucleus (IRF3 and IRF9 along with STAT1) bind to upstream interferon stimulated responsive elements (ISREs) of ISGs and bring about the transcription of ISGs (Schmid et al., 2010). Once outside the nucleus and translated, proteins – ISGs, and IRFs act synergistically (Zhang et al., 2013). ISG15 brings about the ISGylation of IRF3 (Shi et al., 2010). ISGs Mx1, Mx2, OAS1X, OAS1Y, OAS1Z, RSAD2, IFIT3 (ISG58), IFIT5 (ISG60), IFITM2 and IFITM3 expressed/activated by IRFs (IRF- 3, 7 & 9) in the present study help in inducing a broad-spectrum anti-viral state (Schneider et al., 2014; Siddappa Manjunath et al., 2015). The expression of IRF3, IRF7, IFIT3, ISG15, and HERC5 was validated by q-RTPCR and found in concordance with the RNA sequencing results.

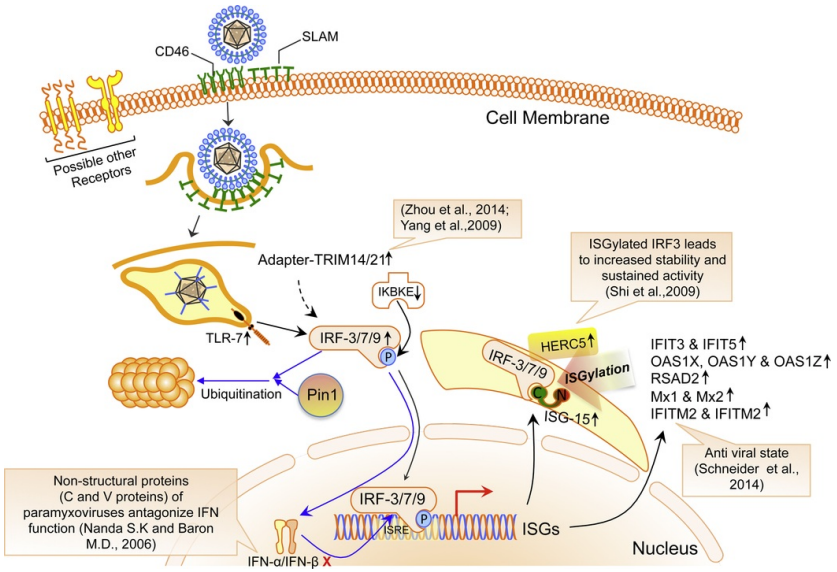

Fig. 7 Predicted immune signaling pathway in PBMCs infected Sungri/96 vaccine virus: The PPR virus enters the PBMCs through specific receptors (SLAM/CD46). After entry, the virus is endocytosed and the viral nucleic acid (ssRNA) released is engaged b TLR7, which induces the expression of interferon regulatory factors IRFs – 3, 7 and 9. The IRFs expressed are phosphorylated and activated by IKBKE. This activation is mediated by adapters – TRIM14/21. The activated IRFs translocate into the nucleus, anc bind to the ISRE (Interferon stimulated responsive elements) upstream of ISGs resulting in their expression. ISG15 ISGylates IRF3, catalysed by HERC5 for its sustained action. ISGs – Mx1, Mx2, OAS1X, OAS1Y, OAS1Z, RSAD2, IFIT3 (ISG58), IFIT5 (ISG60) IFITM2 and IFITM3 expressed in the study bring about a broad-spectrum anti-viral response. The path represented by black arrows is the predicted pathway and the path represented by blue arrows is the pathway that is not followed. Up and down arrows by the side of gene names indicate upregulation and downregulation in RNA sequencing analysis, respectively. The expression of IRF3, IRF7, IFIT3, ISG15, and HERC5 was validated by qRT-PCR and was in concordance with the RNA sequencing results. The crossmark in red indicates absence of expression. (For interpretation of the references to colour in this figure legend, the reader is referred to the web version of this article.)

alt-text: Fig. 7

5 Conclusion

In summary, this time point study highlighted activation of host TLRs and interferon regulatory factors, which further resulted in induction of interferon induced genes in an interferon independent manner at early time points. Anti-viral response induced by Sungri/96 involved both innate and adaptive immune systems with the enrichment of complement cascade observed at 120 h p.i.

Conflict of interest

The authors declare no conflict of interest.

Acknowledgements

This study was supported in part by Department of Biotechnology (BT/PR7729/AAQ/1/542/2013), Government of India and qRT-PCR was done partly from the funds of Centre for Agricultural Bioinfomatics (ICAR-IASRI).

Appendix A. Supplementary data

Supplementary data associated with this article can be found, in the online version, at http://dx.doi.org/10.1016/j.virusres.2016.12.014.

References

Adombi C.M., Lelenta M., Lamien C.E., Shamaki D., Koffi Y.M., Traore A., Silber R., Couacy-Hymann E., Bodjo S.C., Djaman J.A., Luckins A.G. and Diallo A., Monkey CV1 cell line expressing the sheep-goat SLAM

protein: a highly sensitive cell line for the isolation of peste des petits ruminants virus from pathological specimens, *J. Virol. Methods* **173** (2), 2011, 306–313.

Akira S., Uematsu S. and Takeuchi O., Pathogen recognition and innate immunity, *Cell* **124** (4), 2006, 783–801.

Albina E., Kwiatek O., Minet C., Lancelot R., Servan de Almeida R. and Libeau G., Peste des Petits Ruminants, the next eradicated animal disease?, *Vet. Microbiol.* **165** (1–2), 2013, 38–44.

Alexopoulou L., Holt A.C., Medzhitov R. and Flavell R.A., Recognition of double-stranded RNA and activation of NF-kappaB by Toll-like receptor 3, *Nature* **413** (6857), 2001, 732–738.

Bailey T.L., Williams N., Misleh C. and Li W.W., MEME: discovering and analyzing DNA and protein sequence motifs, *Nucleic Acids Res* **34** (Web Server issue), 2006, W369–W373.

Banyard A.C., Parida S., Batten C., Oura C., Kwiatek O. and Libeau G., Global distribution of peste des petits ruminants virus and prospects for improved diagnosis and control, *J. Gen. Virol.* **91** (Pt 12), 2010, 2885–2897.

Bindea G., Mlecnik B., Hackl H., Charoentong P., Tosolini M., Kirilovsky A., Fridman W.H., Pages F., Trajanoski Z. and Galon J., ClueGO: a Cytoscape plug-in to decipher functionally grouped gene ontology and pathway annotation networks, *Bioinformatics* **25** (8), 2009, 1091–1093.

Bolt G., Berg K. and Blixenkrone-Moller M., Measles virus-induced modulation of host-cell gene expression, *J. Gen. Virol.* **83** (Pt 5), 2002, 1157–1165.

Boon A.C., Finkelstein D., Zheng M., Liao G., Allard J., Klumpp K., Webster R., Peltz G. and Webby R.J., H5N1 influenza virus pathogenesis in genetically diverse mice is mediated at the level of viral load, *MBio* **2** (5), 2011.

Boxer E.L., Nanda S.K. and Baron M.D., The rinderpest virus non-structural C protein blocks the induction of type 1 interferon, *Virology* **385** (1), 2009, 134–142.

Chakrabarti A.K., Vipat V.C., Mukherjee S., Singh R., Pawar S.D. and Mishra A.C., Host gene expression profiling in influenza A virus-infected lung epithelial (A549) cells: a comparative analysis between highly pathogenic and modified H5N1 viruses, *Virol. J.* **7**, 2010, 219.

Collins S.E., Noyce R.S. and Mossman K.L., Innate cellular response to virus particle entry requires IRF3 but not virus replication, *J. Virol.* **78** (4), 2004, 1706–1717.

Dhanasekaran S., Biswas M., Vignesh A.R., Ramya R., Raj G.D., Tirumurugaan K.G., Raja A., Kataria R.S., Parida S. and Subbiah E., Toll-like receptor responses to Peste des petits ruminants virus in goats and water buffalo, *PLoS One* **9** (11), 2014, e111609.

Diallo A., Barrett T., Barbron M., Subbarao S.M. and Taylor W.P., Differentiation of rinderpest and peste des petits ruminants viruses using specific cDNA clones, *J. Virol. Methods* **23** (2), 1989, 127–136.

Diebold S.S., Kaisho T., Hemmi H., Akira S. and Reis e Sousa C., Innate antiviral responses by means of TLR7-mediated recognition of single-stranded RNA, *Science* **303** (5663), 2004, 1529–1531.

Durfee L.A., Lyon N., Seo K. and Huibregtse J.M., The ISG15 conjugation system broadly targets newly synthesized proteins: implications for the antiviral function of ISG15, *Mol. Cell* **38** (5), 2010, 722–732.

Fontanesi L., Martelli P.L., Beretti F., Riggio V., Dall'Olio S., Colombo M., Casadio R., Russo V. and Portolano B., An initial comparative map of copy number variations in the goat (Capra hircus) genome, *BMC Genomics* **11**, 2010, 639.

Gack M.U., Kirchhofer A., Shin Y.C., Inn K.S., Liang C., Cui S., Myong S., Ha T., Hopfner K.P. and Jung J.U., Roles of RIG-I N-terminal tandem CARD and splice variant in TRIM25-mediated antiviral signal transduction, *Proc. Natl. Acad. Sci. U. S. A.* **105** (43), 2008, 16743–16748.

Girardin S.E., Sansonetti P.J. and Philpott D.J., Intracellular vs extracellular recognition of pathogens–common concepts in mammals and flies, *Trends Microbiol.* **10** (4), 2002, 193–199.

Gupta S., Stamatoyannopoulos J.A., Bailey T.L. and Noble W.S., Quantifying similarity between motifs, *Genome Biol.* **8** (2), 2007, R24.

Harty R.N., Pitha P.M. and Okumura A., Antiviral activity of innate immune protein ISG15, *J. Innate Immun.* **1** (5), 2009, 397–404.

Hiscott J., Triggering the innate antiviral response through IRF-3 activation, *J. Biol. Chem.* **282** (21), 2007, 15325–15329.

Hsu Y.L., Shi S.F., Wu W.L., Ho L.J. and Lai J.H., Protective roles of interferon-induced protein with tetratricopeptide repeats 3 (IFIT3) in dengue virus infection of human lung epithelial cells, *PLoS One* **8** (11), 2013, e79518.

Huang da W., Sherman B.T. and Lempicki R.A., Systematic and integrative analysis of large gene lists using DAVID bioinformatics resources, *Nat. Protoc.* **4** (1), 2009, 44–57.

Hummel M., Bonnin S., Lowy E. and Roma G., TEQC: an R package for quality control in target capture experiments, *Bioinformatics* **27** (9), 2011, 1316–1317.

Iwasa T., Suga S., Qi L. and Komada Y., Apoptosis of human peripheral blood mononuclear cells by wild-type measles virus infection is induced by interaction of hemagglutinin protein and cellular receptor, SLAM via caspase-dependent pathway, *Microbiol. Immunol.* **54** (7), 2010, 405–416.

Jensen S. and Thomsen A.R., Sensing of RNA viruses: a review of innate immune receptors involved in recognizing RNA virus invasion, *J. Virol.* **86** (6), 2012, 2900–2910.

Jin S. and Zou X., Construction of the influenza A virus infection-induced cell-specific inflammatory regulatory network based on mutual information and optimization, *BMC Syst. Biol.* **7**, 2013, 105.

Kim D., Pertea G., Trapnell C., Pimentel H., Kelley R. and Salzberg S.L., TopHat2: accurate alignment of transcriptomes in the presence of insertions, deletions and gene fusions, *Genome Biol.* **14** (4), 2013, R36.

Kohane I.S. and Valtchinov V.I., Quantifying the white blood cell transcriptome as an accessible window to the multiorgan transcriptome, *Bioinformatics* **28** (4), 2012, 538–545.

Kuchipudi S.V., Tellabati M., Sebastian S., Londt B.Z., Jansen C., Vervelde L., Brookes S.M., Brown I.H., Dunham S.P. and Chang K.C., Highly pathogenic avian influenza virus infection in chickens but not ducks is associated with elevated host immune and pro-inflammatory responses, *Vet. Res.* **45**, 2014, 118.

Kumar K.S., Babu A., Sundarapandian G., Roy P., Thangavelu A., Kumar K.S., Arumugam R., Chandran N.D., Muniraju M., Mahapatra M., Banyard A.C., Manohar B.M. and Parida S., Molecular characterisation of lineage IV peste des petits ruminants virus using multi gene sequence data, *Vet. Microbiol.* **174** (1–2), 2014a, 39–49.

Kumar N., Maherchandani S., Kashyap S.K., Singh S.V., Sharma S., Chaubey K.K. and Ly H., Peste des petits ruminants virus infection of small ruminants: a comprehensive review, *Viruses* **6** (6), 2014b, 2287–2327.

Kwiatek O., Ali Y.H., Saeed I.K., Khalafalla A.I., Mohamed O.I., Obeida A.A., Abdelrahman M.B., Osman H.M., Taha K.M., Abbas Z., El Harrak M., Lhor Y., Diallo A., Lancelot R., Albina E. and Libeau G., Asian lineage of peste des petits ruminants virus, Africa, *Emerg. Infect. Dis.* **17** (7), 2011, 1223–1231.

Langmead B. and Salzberg S.L., Fast gapped-read alignment with Bowtie 2, *Nat. Methods* **9** (4), 2012, 357–359.

Lazear H.M., Lancaster A., Wilkins C., Suthar M.S., Huang A., Vick S.C., Clepper L., Thackray L., Brassil M.M., Virgin H.W., Nikolich-Zugich J., Moses A.V., Gale M., Jr., Fruh K. and Diamond M.S., IRF-3, IRF-5, and IRF-7 coordinately regulate the type I IFN response in myeloid dendritic cells downstream of MAVS signaling, *PLoS Pathog.* **9** (1), 2013, e1003118.

Lee S.M., Kok K.H., Jaume M., Cheung T.K., Yip T.F., Lai J.C., Guan Y., Webster R.G., Jin D.Y. and Peiris J.S., Toll-like receptor 10 is involved in induction of innate immune responses to influenza virus infection, *Proc. Natl. Acad. Sci. U. S. A.* **111** (10), 2014, 3793–3798.

Liew C.C., Ma J., Tang H.C., Zheng R. and Dempsey A.A., The peripheral blood transcriptome dynamically reflects system wide biology: a potential diagnostic tool, *J. Lab. Clin. Med.* **147** (3), 2006, 126–132.

Liu H., Wang T., Wang J., Quan F. and Zhang Y., Characterization of Liaoning cashmere goat transcriptome: sequencing, de novo assembly, functional annotation and comparative analysis, *PLoS One* **8** (10), 2013, e77062

Manjunath S., Kumar G., Mishra B., Mishra B., Sahoo A., Joshi C.G., Tiwari A.K., Rajak K. and Janga S., Genomic analysis of host—Peste des petits ruminants vaccine viral transcriptome uncovers transcription factors modulating immune regulatory pathways, *Vet. Res.* **46** (1), 2015, 15.

McNab F.W., Rajsbaum R., Stoye J.P. and O'Garra A., Tripartite-motif proteins and innate immune regulation, *Curr. Opin. Immunol.* **23** (1), 2011, 46–56.

Nanda S.K. and Baron M.D., Rinderpest virus blocks type I and type II interferon action: role of structural and nonstructural proteins, *J. Virol.* **80** (15), 2006, 7555–7568.

Osiak A., Utermohlen O., Niendorf S., Horak I. and Knobeloch K.P., ISG15, an interferon-stimulated ubiquitin-like protein, is not essential for STAT1 signaling and responses against vesicular stomatitis and lymphocytic choriomeningitis virus, *Mol. Cell. Biol.* **25** (15), 2005, 6338–6345.

Patel R.K. and Jain M., NGS QC Toolkit: a toolkit for quality control of next generation sequencing data, *PLoS One* **7** (2), 2012, e30619.

Pawar R.M., Dhinakar Raj G. and Balachandran C., Relationship between the level of signaling lymphocyte activation molecule mRNA and replication of Peste-des-petits-ruminants virus in peripheral blood mononuclear cells of host animals, *Acta Virol~~ogica~~.* **52** (4), 2008, 231–236.

Reimand J., Arak T. and Vilo J., g:Profiler—a web server for functional interpretation of gene lists, *Nucleic Acids Res.* **39** (Web Server issue), 2011, W307–W315, 2011 update.

Sadler A.J. and Williams B.R., Interferon-inducible antiviral effectors, *Nat. Rev. Immunol.* **8** (7), 2008, 559–568.

Saravanan P., Sen A., Balamurugan V., Rajak K.K., Bhanuprakash V., Palaniswami K.S., Nachimuthu K., Thangavelu A., Dhinakarraj G., Hegde R. and Singh R.K., Comparative efficacy of peste des petits ruminants (PPR) vaccines, *Biologicals* **38** (4), 2010, 479–485.

Schmid S., Mordstein M., Kochs G., Garcia-Sastre A. and Tenoever B.R., Transcription factor redundancy ensures induction of the antiviral state, *J. Biol. Chem.* **285** (53), 2010, 42013–42022.

Schmieder R. and Edwards R., Quality control and preprocessing of metagenomic datasets, *Bioinformatics* **27** (6), 2011, 863–864.

Schmittgen T.D. and Livak K.J., Analyzing real-time PCR data by the comparative C(T) method, *Nat. Protoc.* **3** (6), 2008, 1101–1108.

Schneider W.M., Chevillotte M.D. and Rice C.M., Interferon-stimulated genes: a complex web of host defenses, *Annu. Rev. Immunol.* **32**, 2014, 513–545.

Sen G.C. and Sarkar S.N., The interferon-stimulated genes: targets of direct signaling by interferons, double-stranded RNA, and viruses, *Curr. Top. Microbiol. Immunol.* **316**, 2007, 233–250.

Shannon P., Markiel A., Ozier O., Baliga N.S., Wang J.T., Ramage D., Amin N., Schwikowski B. and Ideker T., Cytoscape: a software environment for integrated models of biomolecular interaction networks, *Genome Res.* **13** (11), 2003, 2498–2504.

Shi H.X., Yang K., Liu X., Liu X.Y., Wei B., Shan Y.F., Zhu L.H. and Wang C., Positive regulation of interferon regulatory factor 3 activation by Herc5 via ISG15 modification, *Mol. Cell. Biol.* **30** (10), 2010, 2424–2436.

Siddappa Manjunath B.M., Prasad Mishra Bishnu, Saxena Shikha, Mondal Piyali, Ranjan Sahu Amit, Prasad Sahoo Aditya, Tiwari Ashok K. and Gandham Ravi Kumar, Identification of suitable reference gene in goat peripheral blood mononuclear cells (PBMCs) infected with peste des petits ruminants virus (PPRV), *Livest. Sci.* **181**, 2015, 15–155.

Singh R.P., Sreenivasa B.P., Dhar P., Shah L.C. and Bandyopadhyay S.K., Development of a monoclonal antibody based competitive-ELISA for detection and titration of antibodies to peste des petits ruminants (PPR) virus, *Vet. Microbiol.* **98** (1), 2004, 3–15.

Singh R.K., Balamurugan V., Bhanuprakash V., Sen A., Saravanan P. and Pal Yadav M., Possible control and eradication of peste des petits ruminants from India: technical aspects, *Vet. Ital.* **45** (3), 2009, 449–462.

Singh R.P., De U.K. and Pandey K.D., Virological and antigenic characterization of two Peste des Petits Ruminants (PPR) vaccine viruses of Indian origin, *Comp. Immunol. Microbiol. Infect. Dis.* **33** (4), 2010, 343–353.

Sinnathamby G., Renukaradhya G.J., Rajasekhar M., Nayak R. and Shaila M.S., Immune responses in goats to recombinant hemagglutinin-neuraminidase glycoprotein of Peste des petits ruminants virus: identification o a T cell determinant, *Vaccine* **19** (32), 2001, 4816–4823.

Stark C., Breitkreutz B.J., Reguly T., Boucher L., Breitkreutz A. and Tyers M., BioGRID: a general repository for interaction datasets, *Nucleic Acids Res.* **34** (Database issue), 2006, D535–D539.

Tatsuo H. and Yanagi Y., The morbillivirus receptor SLAM (CD150), *Microbiol. Immunol.* **46** (3), 2002, 135–142.

Trapnell C., Roberts A., Goff L., Pertea G., Kim D., Kelley D.R., Pimentel H., Salzberg S.L., Rinn J.L. and Pachter L., Differential gene and transcript expression analysis of RNA-seq experiments with TopHat and Cufflinks, *Nat. Protoc.* **7** (3), 2012, 562–578.

Tsuchida T., Zou J., Saitoh T., Kumar H., Abe T., Matsuura Y., Kawai T. and Akira S., The ubiquitin ligase TRIM56 regulates innate immune responses to intracellular double-stranded DNA, *Immunity* **33** (5), 2010, 765–776.

Vanderven H.A., Petkau K., Ryan-Jean K.E., Aldridge J.R., Jr., Webster R.G. and Magor K.E., Avian influenza rapidly induces antiviral genes in duck lung and intestine, *Mol. Immunol.* **51** (3–4), 2012, 316–324.

Yang K., Shi H.X., Liu X.Y., Shan Y.F., Wei B., Chen S. and Wang C., TRIM21 is essential to sustain IFN regulatory factor 3 activation during antiviral response, *J. Immunol.* **182** (6), 2009, 3782–3792.

Zhang B., Liu X., Chen W. and Chen L., IFIT5 potentiates anti-viral response through enhancing innate immune signaling pathways, *Acta Biochim. Biophys. Sin. (Shanghai)* **45** (10), 2013, 867–874.

Zhao C., Hsiang T.Y., Kuo R.L. and Krug R.M., ISG15 conjugation system targets the viral NS1 protein in influenza A virus-infected cells, *Proc. Natl. Acad. Sci. U. S. A.* **107** (5), 2010, 2253–2258.

Zhou Z., Jia X., Xue Q., Dou Z., Ma Y., Zhao Z., Jiang Z., He B., Jin Q. and Wang J., TRIM14 is a mitochondrial adaptor that facilitates retinoic acid-inducible gene-I-like receptor-mediated innate immune response, *Proc. Natl. Acad. Sci. U. S. A.* **111** (2), 2014, E245–254.

van Gent M., Griffin B.D., Berkhoff E.G., van Leeuwen D., Boer I.G., Buisson M., Hartgers F.C., Burmeister W.P., Wiertz E.J. and Ressing M.E., EBV lytic-phase protein BGLF5 contributes to TLR9 downregulation during productive infection, *J. Immunol.* **186** (3), 2011, 1694–1702.

Appendix A. Supplementary data

The following ~~are~~is Supplementary data to this article:

Multimedia Component 1

Highlights

- Temporal dynamics of immune response in PBMCs infected with Sungri/96 vaccine studied.
- Differentially expressed genes reflected enrichment of Immune response pathways.
- The upregulation of innate immune genes –- IRFs and ISGs identified at early phase.
- Broad-spectrum anti-viral state observed under vaccination.
- Viral transcripts have been quantified in infected PBMCs from the RNA sequencing data.

Queries and Answers

Query: The author names have been tagged as given names and surnames (surnames are highlighted in teal color). Please confirm if they have been identified correctly.
Answer: Yes they are correct

Query: Please check whether all author names and affiliations are correctly linked, and correct if necessary.
Answer: The correct affilation of the co author Y.P Sing is "e" not "1"

Query: Please check the presentation of all affiliations and correct if necessary.
Answer: Incorporate ICAR- at the places mentioned

Query: Please check the address of the corresponding author and correct if necessary.
Answer: it is correct

Query: Please check the presentation of author footnote and correct if necessary.
Answer: correct

Query: Please check the hierarchy of the section headings.
Answer: correct

Query: “Your article is registered as a regular item and is being processed for inclusion in a regular issue of the journal. If this is NOT correct and your article belongs to a Special Issue/Collection

please contact m.vs@elsevier.com immediately prior to returning your corrections.”

Answer: correct

Query: Please check the presentation of Section heading "Conflict of interest" and correct if necessary.

Answer: correct

Query: One or more sponsor names and the sponsor country identifier may have been edited to a standard format that enables better searching and identification of your article. Please check and correct if necessary.

Answer: Yes

Query: Figs. 1,4,5,7 will appear in black and white in print and in color on the web. Based on this, the respective figure captions have been updated. Please check, and correct if necessary.

Answer: correct

Query: Please check the presentation of Table 1, and correct if necessary.

Answer: correct